Half-soliton interaction of population taxis waves in predator-prey systems with pursuit and evasion.

M. A. Tsyganov

Institute of Theoretical and Experimental Biophysics, Pushchino, Moscow Region 142290, Russia

V. N. Biktashev

Department of Mathematical Sciences, University of Liverpool, Liverpool L69 7ZL, UK

(Dated: June 9, 2004)

In this paper, we use numerical simulations to demonstrate a new type of interaction of waves in a mathematical model of ”prey-predator” system with taxis, a “half-soliton” interaction, when of two colliding waves, one annihilates and the other continues to propagate. We show that this effect depends on the “ages”, or, equivalently, “widths’ of the colliding waves. In two spatial dimensions we demonstrate the type of interaction, i.e. annihilation, quasi-soliton or half-soliton, depends not only on curvature and width of the colliding waves, but also on the angle of the collision. When conditions of collision are varying in such a way that only a part of a wave survive the collision, then “taxitons”, compact pieces of solitary waves, may form, which can exist for a significant time.

PACS numbers: 87.10.+e

INTRODUCTION.

In this paper we continue the study of a system of two spatially distributed populations in a “predator-prey” relationship with each other, started in our previous works [1–3]. The spatial evolution is governed by three processes: positive taxis of predators up the gradient of prey (pursuit) and negative taxis of prey down the gradient of predators (evasion), yielding nonlinear “cross-diffusion” terms, and random motion of both species (diffusion). The resulting mathematical model is a system of two partial differential equations,

$$\begin{aligned} \frac{\partial P}{\partial t} &= f(P,Z) + D\nabla^2 P + h_-\nabla\left(P\nabla Z\right), \\ \frac{\partial Z}{\partial t} &= g(P,Z) + D\nabla^2 Z - h_+\nabla\left(Z\nabla P\right), \end{aligned} \tag{1}$$

where $P(\mathbf{r},t)$ is the density of the prey population, $Z(\mathbf{r},t)$ is the density of the predator population, the nonlinear functions $f(P,Z)$ and $g(P,Z)$ describe local dynamics, including growth and interaction of the species, whereas the diffusion terms describe their spread in space, e.g. resulting from individual random motions. The taxis terms are as in [4], constant h_- is the coefficient of negative taxis of P on the gradient of Z (prey evading predators), and h_+ is the coefficient of positive taxis of Z on the gradient of P (predators pursuing prey). For simplicity, the diffusion coefficient D is considered constant, uniform and equal for both species. In this paper we consider problems in one spatial dimension, $\mathbf{r} = (x)$, and in two spatial dimensions, $\mathbf{r} = (x, y)$.

We consider the local kinetics functions $f(P, Z)$ and $g(P, Z)$, describing the population dynamics of prey (phytoplankton) P and predators (zooplankton) Z, in the Holling type III form used by Truscott and Brindley [5]. In non-dimensional form these are

$$
\begin{aligned}
f(P, Z) &= \beta P(1 - P) - ZP^2/(P^2 + \nu^2), \\
g(P, Z) &= \gamma ZP^2/(P^2 + \nu^2) - wZ.
\end{aligned} \tag{2}
$$

It is known that at appropriate choice of parameters, these kinetics demonstrate "excitable" behaviour, and the reaction-diffusion system (1) with $h_- = h_+ = 0$ has propagating solitary wave solutions [5, 6].

We have studied properties of population taxis waves in the mathematical model (1,2) for one dimensional [1, 2] and two dimensional [3] cases. In those works, we have shown that inclusion of the taxis terms can radically change the properties of propagating waves, compared to the much better studied waves in purely reaction-diffusion systems without taxis. We have demonstrated that the very mechanism of propagation of waves in such systems is different. Here are some peculiar features of taxis waves, described in [1, 2]:

- (a) Essentially different shape of the wave profiles. For $P(x - ct)$ profile, it could be either "single-hump" or "double-hump" shape.
- (b) The dependence of the wave propagating velocity on the taxis coefficients has two distinct branches, "parabolic" and "linear". The transition from one branch to the other correlates with changes in the shape of the wave profiles: the parabolic branch of this graph correspond to a "double-hump" shape of the $P(x - ct)$ profile, and the linear branch corresponds to a "single-hump" shape.
- (c) In the space of parameters of (1), there are large regions, where waves demonstrate quasi-soliton interaction: they can penetrate through each other, and also reflect from impermeable boundaries, see Fig. 1(a-c).
- (d) For some regions in the parameter space, taxis waves can spontaneously split, emitting "backward" propagating waves. This can be observed both in the case of soliton-like interaction (Fig. 1(a), solid triangles) and in the case of annihilating

waves (Fig. 1(a), hollow triangles). The backward emitted waves with time either decay, or split themselves. In the latter case, the chain of splitting events can lead to self-supporting, aperiodic or approximately periodic activity.

- (e) The dependence of the propagation velocity on diffusion in this system differs from the square-root dependence, always valid for reaction-diffusion waves, see Fig. 1(d).

  Additionally, in two spatial dimensions, we observed [3]

- (f) Partial reflection of waves from boundaries, or their partial penetration through each other.
- (g) "Swollen tips", i.e. circular wave sources, produced by free ends of broken waves.
- (h) Attachment of free ends of broken waves to the wavebacks.

In this paper, by numerical simulation of the system (1,2) we demonstrate a new type wave interactions, when of two colliding waves, one annihilates and the other continues to propagate. For brevity, we call this behaviour "half-soliton".

DETAILS OF THE MODEL AND NUMERICAL METHODS

We used "upwind" schemes to approximate the taxis terms $\mathcal{L}u = \frac{\partial}{\partial x}u(x,t)\frac{\partial S(x,t)}{\partial x}$. The idea of the "upwind" schemes is that they use not the mean between values of the variables subject to taxis at two neighbouring grid nodes as in the central scheme, but select one or the other depending on the direction of taxis, i.e. sign of the gradient of the attractant. For details of the schemes we used, see our previous work [2]. As we have shown in [2], the implicit central scheme only works for (1) if $D > 0$, whereas our "upwind" schemes work for $D = 0$ as well. We used time-implicit scheme with discretization steps $\delta x = 0.1$, and $\delta t = 5 \times 10^{-3}$ for one-dimensional simulations, and time-explicit with discretization steps for $\delta x = \delta y = 0.5$ and $\delta t = 5 \times 10^{-3}$ for two-dimensional calculations.

Unless specified otherwise, we have used the same parameters in (1) in our numerics, as we used in [2], that is $\beta = 1$, $\nu = 0.07$, $w = 0.004$, and two different values of γ: $\gamma = 0.01$, henceforth "small γ", which allows propagation of purely reaction-diffusion waves, i.e. with $h_+ = h_- = 0$, $D > 0$; and $\gamma = 0.016$, henceforth "large γ", for which purely reaction-diffusion waves do not propagate, and taxis is required (see Fig. 1(a-c)). *System (**??**) non-dimensionalized, thus all the variables and parameters are dimensionless.*

In all numerics, we used non-flux boundary conditions: $\frac{\partial P}{\partial x}|_{x=0,L} = 0$ and $\frac{\partial Z}{\partial x}|_{x=0,L} = 0$ for one-dimensional problems, $x \in [0, L]$, and $\frac{\partial P}{\partial x}|_{x=0,L_x} = 0$, $\frac{\partial Z}{\partial x}|_{x=0,L_x} = 0$ and $\frac{\partial P}{\partial y}|_{y=0,L_y} = 0$, $\frac{\partial Z}{\partial y}|_{y=0,L_y} = 0$ for two-dimensional problems, $(x, y) \in$

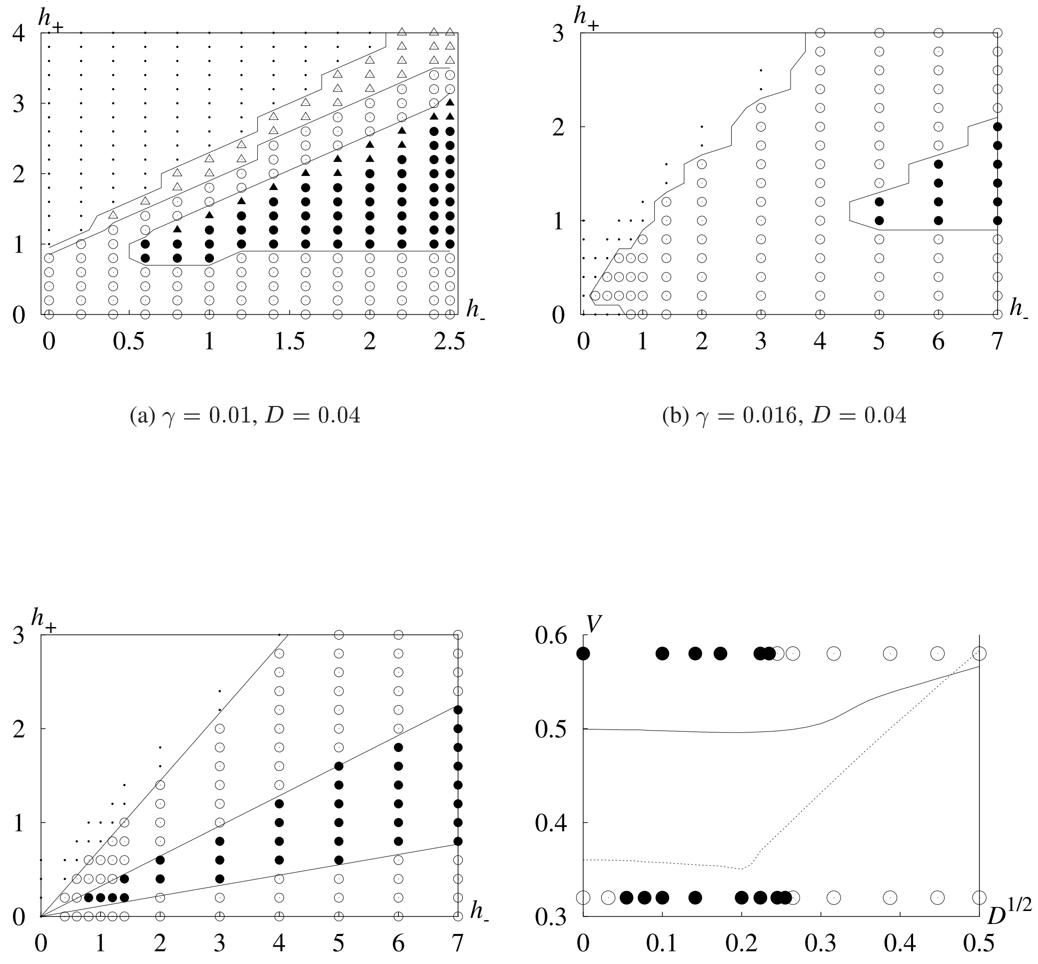

(a) $\gamma = 0.01$, $D = 0.04$

(b) $\gamma = 0.016$, $D = 0.04$

(c) $\gamma = 0.016$, $D = 0$

(d)

FIG. 1: (a), (b), (c) Parametric regions corresponding to different regimes of taxis waves ($\beta = 1$, $w = 0.004$). Solid circles: quasi-soliton waves. Solid triangles: quasi-solitons with the wave splitting. Hollow circles: stably propagating waves annihilating on collision. Hollow triangles: splitting waves annihilating on collision. Dots: no propagating wave solution. (d) Wave propagation velocity as function of the square root of the diffusion coefficient. Solid line and the upper row of symbols: $\gamma = 0.016$, $h_- = 5$, $h_+ = 1$. Dotted line and the lower row: $\gamma = 0.01$, $h_- = h_+ = 1$. In reaction-diffusion systems, this dependence is always a straight line. *Here and on other figures, all parameters and variables are dimensionless.*

$[0, L_x] \times [0, L_y]$.

"HALF-SOLITON" WAVE INTERACTION IN ONE DIMENSIONAL CASE

Figure 2 illustrates spatio-temporal dynamics of population taxis waves in (1), including their formation, propagation and reflection from boundaries. The waves were initiated, both for small γ, panel (a), and for large γ, panel (b), by setting initial conditions for $P(x, 0) = 0.8$ for $x \in [0, 1]$ and $P(x, 0)$ for $x \in (1, L]$ and $Z(x, 0)$ for $x \in [0, L]$ equal to their equilibrium values.

The key observation for the present paper is that taxis waves establish their stationary structure and corresponding speed only after a rather long transient. Figure 3 illustrates variations of the propagation velocity, V, panels (a,c) and width, W, panel (b,d), of a wave during such transients, both before and after its reflection from the boundary. During the transient, the propagation velocity distinctly decreases for a short interval of time (approximately between $t = 450$ and $t = 550$), while the wave width continues to monotonically approach its stationary value. This temporary decrease of the velocity correlates with a change in the shape of the wave profile. Figures 4 and 5 show the wave profiles corresponding to selected time moments, indicated by arrows on Fig. 3. We see that the temporary decrease of propagation velocity corresponds to the transition of the wave profile from double-hump to single-hump shape. As mentioned earlier, in [2] we have shown that these two shapes correspond to two distinct branches on the graph of stationary propagation speed V on h_+, "parabolic" and "linear". Figures 4 and 5 demonstrate that the transition from one shape to the other happens during the transient, thus associated variations in the propagation velocity seen on Fig. 3. Besides, the change of shape itself causes apparent short-term change in the velocity due to the method of the measuring the velocity of the wave, as the velocity of the point with a particular value of P; this is the main reason with the sharp local minima of the propagation velocity coinciding with the transitions from one wave shape to the other.

On the other hand, the type of interaction of stationary waves, i.e. reflection or annihilation (see Fig. 1), also correlates with the shape of the profiles of those waves [2]. Since the shape of the profiles changes in the long transient after the wave initiation, we decided to check if the waves at different stages of their "life" will show different type of interaction, corresponding to their current shape. This conjecture has been tested by numerical experiments, results of which are presented on Fig. 6. Periodic waves were initiated in a one-dimensional medium with non-flux boundaries. In addition to already known quasi-soliton reflection of waves and their splitting, we have observed also a new type of interaction, where of two colliding waves only one survives, whereas the other decays. We call this "half-soliton" interaction.

For a detailed study of this half-soliton interaction, we simulated collisions of artificially prepared taxis waves of different "ages". We have recorded a wave in a large medium at chosen moments of its transient, namely, $t = 195, 345, 461$ and 645; (all

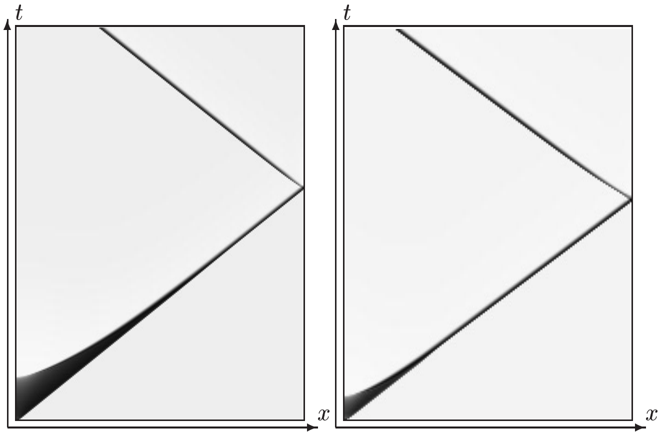

(a) $t \in [0, 1200]$ (b) $t \in [0, 900]$

FIG. 2: The spatio-temporal dynamics of the taxis wave formation, propagation and reflection from impermeable boundaries for system (1) in one dimensional case with $L = 250$: (a)$\gamma = 0.01$, $D = 0.04$, $h_- = h_+ = 1$; (b)$\gamma = 0.016$, $D = 0$, $h_- = 5, h_+ = 1$. Black corresponds to $P = 0.9$, white to $P = 0$.

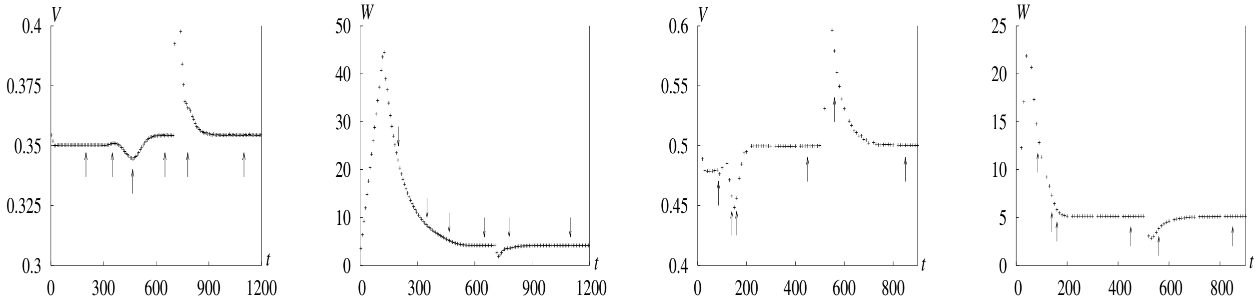

(a) (b) (c) (d)

FIG. 3: Variations of the propagation velocity (a,c) and wave width (b,d) during the transient, corresponding to Fig. 2: (a,b) $\gamma = 0.01$, $D = 0.04$, $h_- = h_+ = 1$, (c,d) $\gamma = 0.016$, $D = 0$, $h_- = 5, h_+ = 1$. Width $W(t)$ is defined as the distance between the points on the front and the back of the wave where $P(x,t) = 0.4$; propagation velocity $V(x,t)$ is defined as the instant velocity of such point on the front, i.e. where $P(x,t) = 0.4$ and $\partial P/\partial t(x,t) > 0$. Arrows designate the time moments, for which Figs. 4 and 5 show the wave profiles.

by 5 time units earlier than the moments shown on Fig. 4). Then we set up initial conditions, in which in one half of the medium we used a recorded wave of one age, suitably shifted along x axis, and in the other half of the medium we used another recorded wave. Of course, the wave in the right half of the medium was also inverted, so as to move towards the left wave. As the time from such artificial initial conditions to the collision was approximately 5 time units, the ages of waves at the very moment of collision correspond to those shown on Fig. 4. So, we denote such waves as as W_{200}, W_{350}, W_{466} and W_{650}, according to their ages.

Figure 7 describes interaction of waves W_{200} and W_{466}. The result is that W_{200} has suppressed W_{466}. Similar events are

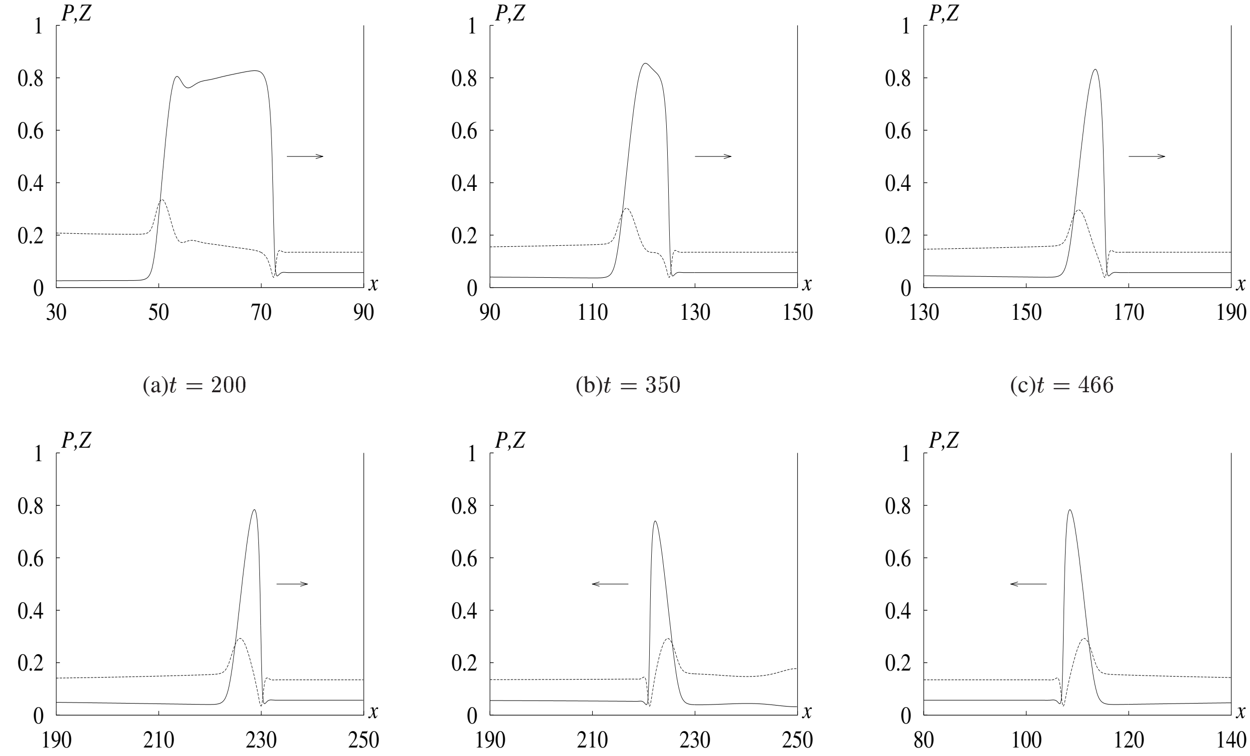

(a)$t = 200$ (b)$t = 350$ (c)$t = 466$

(d)$t = 650$ (e)$t = 780$ (f)$t = 1100$

FIG. 4: Variations of the wave profiles, corresponding to the selected time moments on Fig. 2(a) and Fig. 3(a,b).

	A	B	C	D
A	-	A	A	A
B	A	+	B	B
C	A	B	+	+
D	A	B	+	+

TABLE I: Results of collisions for $\gamma = 0.01$, $D = 0.04$, $h_- = h_+ = 1$. Here 'A' denotes W_{200}, 'B' is W_{350}, 'C' is W_{466}, 'D' is W_{650}, result of collision is shown on the intersection of corresponding row and column, letter denotes the surviving wave, '+' means both waves survive, '-' means neither survives. Approximate ratios of widths ($P = 0.4$) are: $\lambda_A/\lambda_D = 5.3$, $\lambda_B/\lambda_D = 2$, $\lambda_C/\lambda_D = 1.25$.

shown on Fig. 8 (W_{200} vs W_{466}), Fig. 9 (W_{350} vs W_{466}) and Fig. 10 (W_{650} vs W_{466}). Tables I and II summarize the results of collisions of waves of various ages.

These results suggest that the half-soliton interaction takes place when the two colliding waves are essentially different in their widths. A thinner, older wave is less likely to penetrate through a younger, thicker wave. Note, that since the colliding waves now are different from each other, we can distinguish "reflection" from "penetration" of the waves, and the most natural

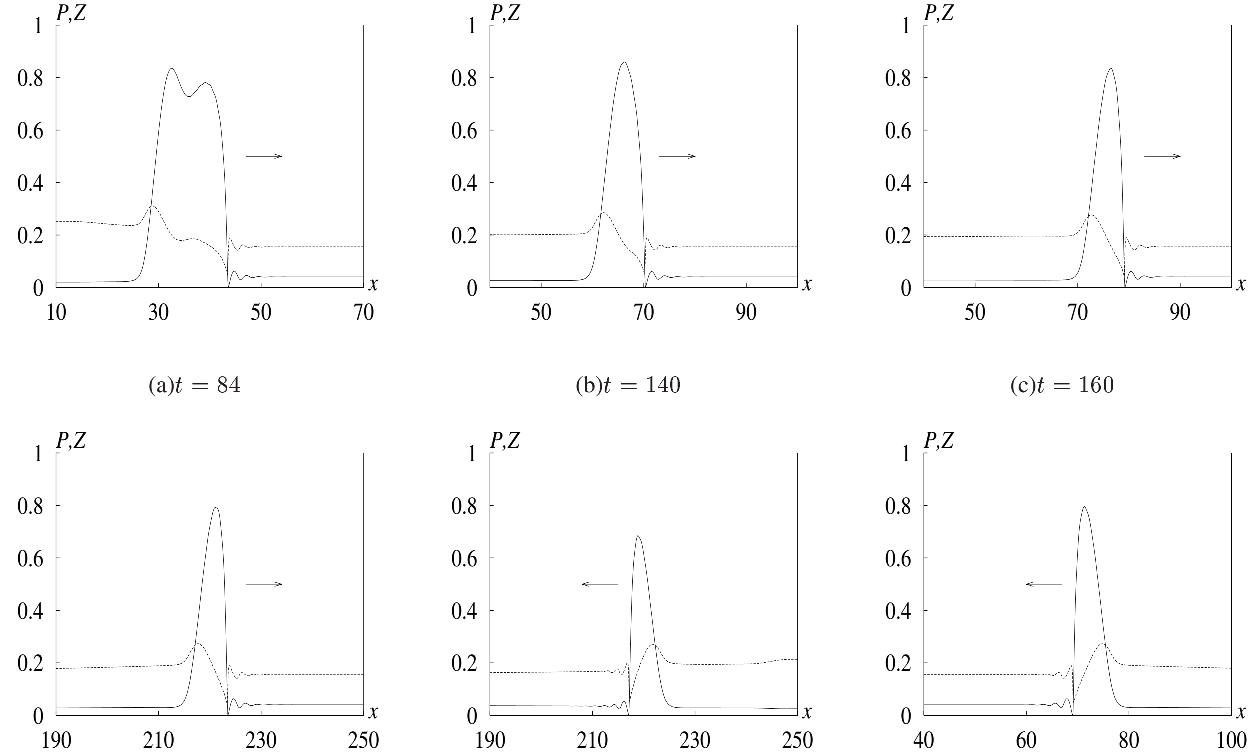

(a)$t = 84$ (b)$t = 140$ (c)$t = 160$

(d)$t = 450$ (e)$t = 560$ (f)$t = 850$

FIG. 5: Variations of the wave profiles, corresponding to the selected time moments on Fig. 2(b) and Fig. 3(c,d).

	a	b	c	d
a	-	a	a	a
b	a	-	b	b
c	a	b	+	+
d	a	b	+	+

TABLE II: Results of collisions for $\gamma = 0.016$, $D = 0$, $h_- = 5$, $h_+ = 1$. Here 'a' is w_{84}, 'b' is w_{140} , 'c' is w_{160} , 'd' is w_{450}, corresponding to the selected moments indicated on Fig. 2, see also Fig. 3(c,d). Approximate ratios of widths ($P = 0.4$) are: $\lambda_a/\lambda_d = 2.8$, $\lambda_b/\lambda_d = 1.4$, $\lambda_c/\lambda_d = 1.14$.

interpretation is that the waves penetrate though each other, if they do, rather than reflect.

HALF-SOLITONS IN TWO DIMENSIONS

In our previous work [3], we have described some typical two-dimensional regimes of propagation of taxis waves in (1,2). In particular, we have demonstrated that for parameters corresponding to quasi-soliton behaviour in one dimension, concentric

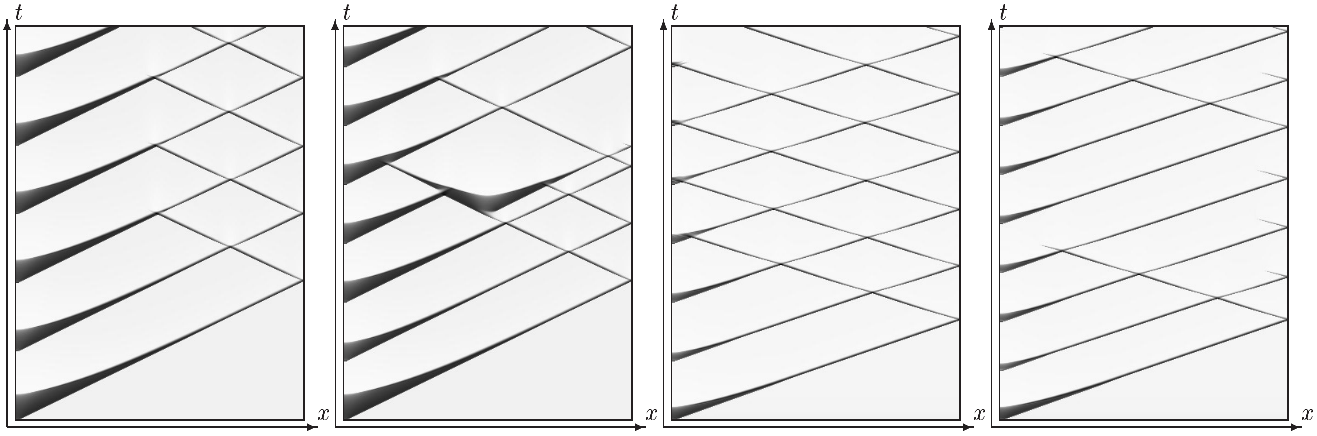

(a) $T = 350$ (b) $T = 300$ (c) $T = 300$ (d) $T = 250$

FIG. 6: The spatio-temporal dynamics of the taxis waves periodically initiated at the left end, with time period T, specified under the density plots. Independent variables ranges: $L = 250$, $t \in [0, 2000]$. (a) and (b): $\gamma = 0.01$, $D = 0.04$, $h_- = h_+ = 1$; (c) and (d): $\gamma = 0.016$, $D = 0$, $h_- = 5$, $h_+ = 1$.

waves can either penetrate/reflect on collision, or annihilate, depending on conditions, particularly on the curvature of the waves. The results of the previous section show, however, that another factor that can affect the result of collision, is the "age" state of the colliding waves.

Let us consider interaction of concentric taxis waves of different radia and different widths. As in one-dimensional collisions, the initial conditions have been prepared from solitary one-dimensional pulses recorded at different stages of their transients and therefore having different widths. If $P_{1d}(x)$, $Z_{1d}(x)$ is such a recording, shifted along x axis so that the front is at $x = 0$, then initial conditions we used can be described as

$$P(x, y, 0) = P_{1d}\left(\sqrt{x^2 + y^2} - R\right), \qquad Z(x, y, 0) = Z_{1d}\left(\sqrt{x^2 + y^2} - R\right),$$

where R was the desired radius of the circular wave.

For parameters $\gamma = 0.016$, $D = 0$, $h_- = 5$, $h_+ = 1$, we initiated a one-dimensional wave in the standard way described above, and recorded it at times $t = 120$ (as wave W), $t = 150$ (wave S) and $t = 450$ (wave U). These recorded waves had widths, measured at level $P = 0.4$, correspondingly, $\lambda_W = 9.2$, $\lambda_S = 6.4$ and $\lambda_U = 5.1$, so that $\lambda_W/\lambda_U = 1.8$ and $\lambda_S/\lambda_U = 1.25$.

Figure 11 shows interaction of two U waves with initial radia $R = 70$. In this case, the waves both penetrate through each other and reflect from the domain boundaries. Similar quasi-soliton interaction is observed on collision of a U and an S waves with equal radia $R = 70$, see Fig. 12. Interaction of U and W waves with the same radia demonstrates a half-soliton behaviour, when wave W suppresses U, but annihilates at the boundary.

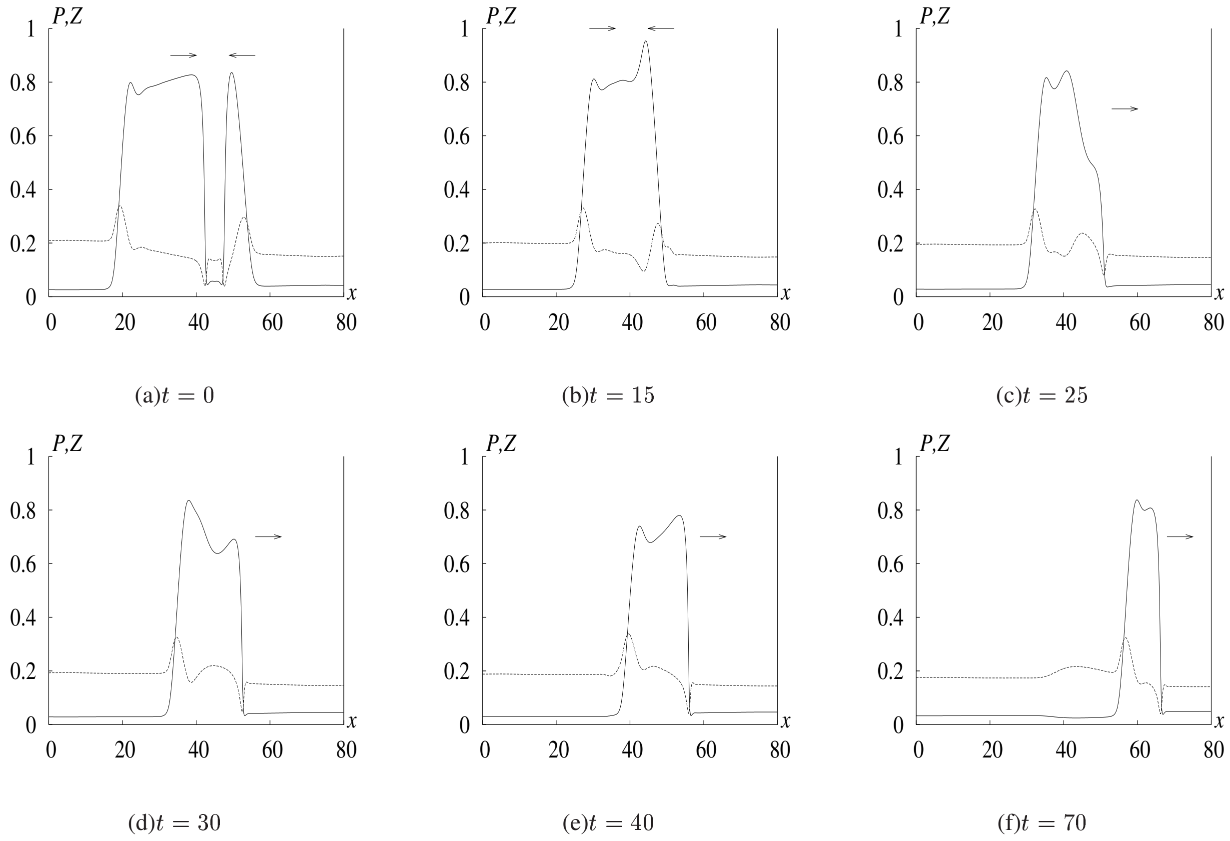

FIG. 7: Collision of W_{200} (from the left) and W_{466} (from the right).

Collision of two S waves with initial radia $R = 40$, see Fig. 14, produces spatially localised waves, which we call “taxitons” (panels d-f). These taxitons interact in half-soliton way with waves reflected from the boundaries (panels g,h).

There are also simulations showing both half-soliton and taxiton regimes at the same time. On Fig. 15, wave U with initial radius $R = 70$ collided with wave S with initial radius $R = 40$. The result was that S-wave penetrated through U in the half-soliton way, and U-wave penetrated only partially, as a taxiton (panels c–e). This is followed by an even more complicated picture of different kinds of interactions, including tip-swelling as described in [3] (panels n,o).

The type of interaction (annihilation, quasi-soliton or half-soliton) depends not only on curvature and width of the colliding waves, but also on the angle of collision. This explains formation of the taxitons, where only a part of a wave continues to propagate after collision, even though all parts of the wave are of the same age. The waves colliding head-on are more likely to penetrate than in a skewed collision, and so when the widths of the waves are close to their critical values allowing penetration, only the part of the wave which is close to first collision site penetrates, whereas more distant parts annihilate.

Figures 16 and 17 illustrate collision at different angles in pure form. Initial conditions have been formed from the same 1D

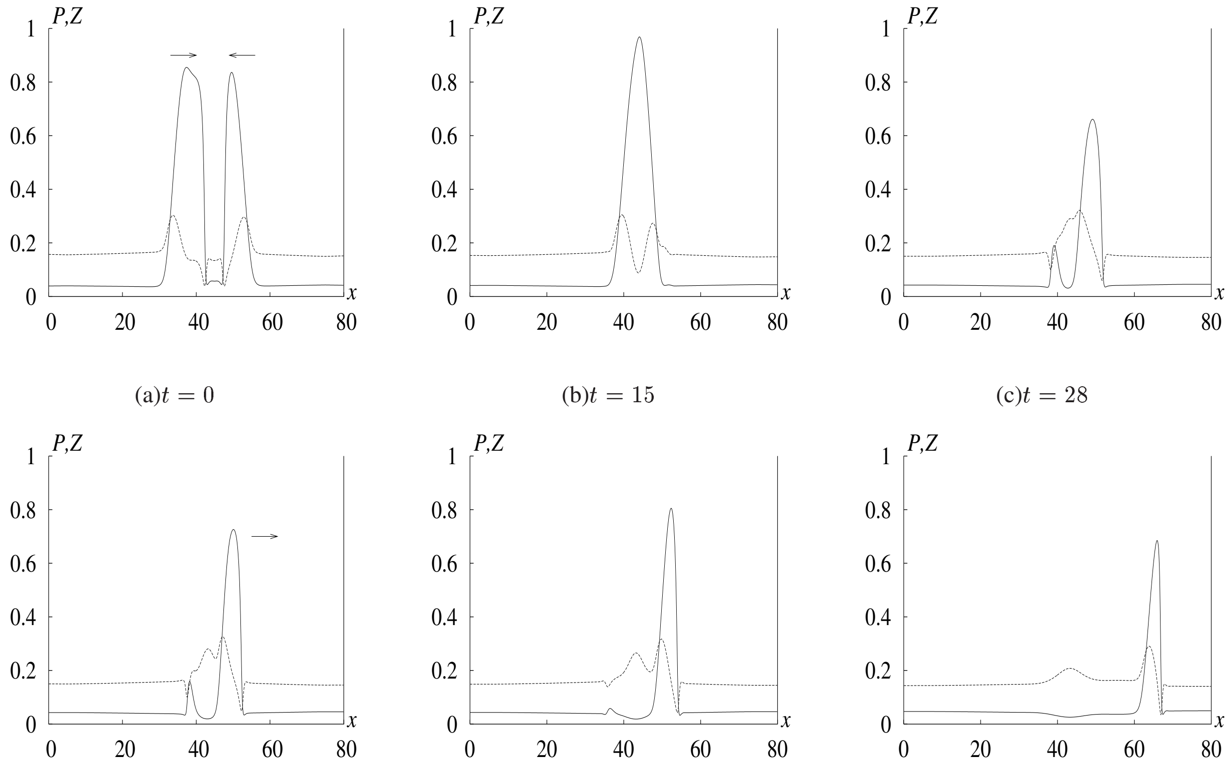

(a)$t = 0$ (b)$t = 15$ (c)$t = 28$

(d)$t = 30$ (e)$t = 35$ (f)$t = 70$

FIG. 8: Collision of W_{350} (from the left) and W_{466} (from the right).

wave U (old-age, well established), arranged in 2D in the form of two plane waves meeting each other at different angles, i.e.

$$P(x, y, 0) = P_{1d}\left(x\cos(\theta) + y\sin(\theta) - C\right), \qquad Z(x, y, 0) = Z_{1d}\left(x\cos(\theta) + y\sin(\theta) - C\right),$$

where θ and C are constants, different for the left and the right halves of the medium.

In Fig. 16, angle between the fronts of the waves is 80°, and the waves annihilate. On Fig. 17, the angle is 60°, and the waves penetrate through each other. This proves directly that result of collision depends on the angle of incidence.

Conclusions. In our previous papers [1–3] we have described soliton-like behaviour and also spontaneous wave splitting in a class of waves that can exist in population dynamics models due to taxis of species to each other's gradients. It was shown that properties of taxis waves are essentially different from those of solitary waves observed in excitable reaction-diffusion systems.

In the present paper we have described new properties of such taxis waves:

- "Half-soliton interaction", when only one of the colliding waves penetrates and the other annihilates. This is observed both in one and in two spatial dimensions.

- "Taxitons", i.e. compact pieces of solitary waves in two dimensions, that can form when only a part of a colliding wave

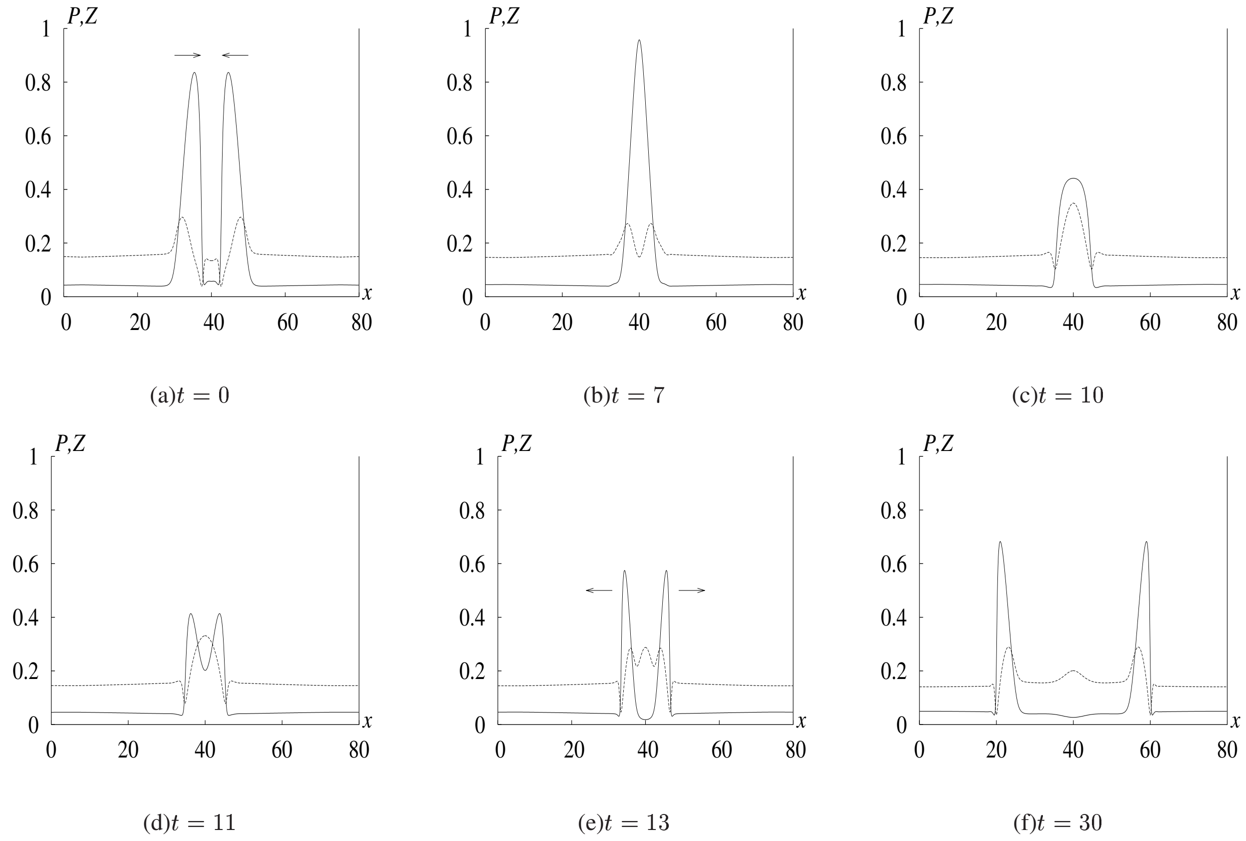

FIG. 9: Collision of W_{466} (from the left) and W_{466} (from the right).

can manage to penetrate through the collision.

We have demonstrated that half-soliton interaction depends on the width of the colliding waves, which can depend on their history, and formation of taxitons depends on that too, and also on the angle of incidence between the colliding waves. The dependence on the angle of incidence is apparently related to the dependence on the wave width, as in an oblique collision, the apparent width of the waves along the line of collision is larger.

So, the results of the present and previous works [1–3] demonstrate that population taxis waves have unique properties, making them different both from solitons in conservative systems [7], and from solitary waves in excitable reaction-diffusion systems [8, 9]. A broader investigation of this new class of nonlinear waves is required, which is both interesting from mathematical viewpoint, and also motivated by recent experimental studies of chemotaxis in bacteria [10, 11], which demonstrated interesting results on propagation and interaction of population taxis waves, and also on self-organisation of population systems with taxis [12–22].

This study was supported in part by EPSRC grant GR/S08664/01 (UK) and RFBR grant 03-01-00673 (Russia).

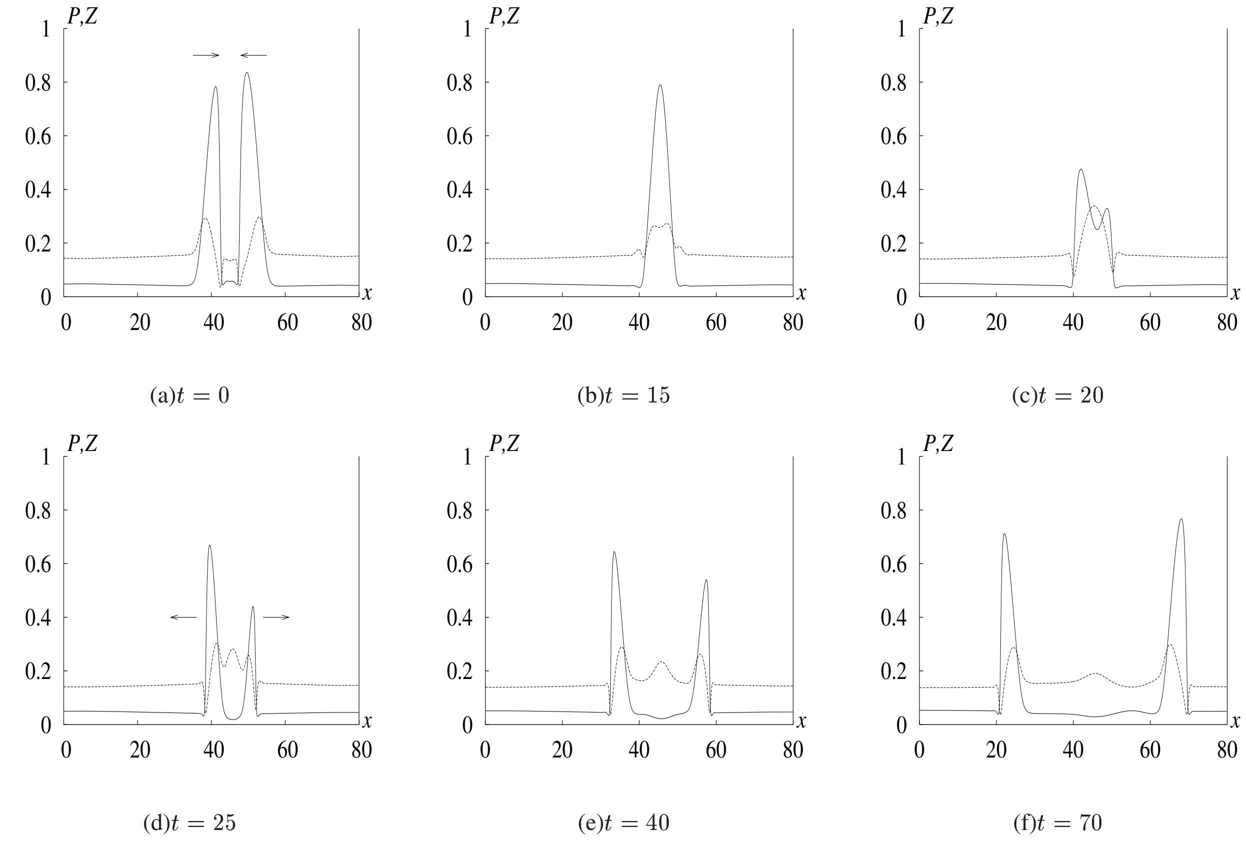

(a)$t = 0$ (b)$t = 15$ (c)$t = 20$

(d)$t = 25$ (e)$t = 40$ (f)$t = 70$

FIG. 10: Collision of W_{650} (from the left) and W_{466} (from the right).

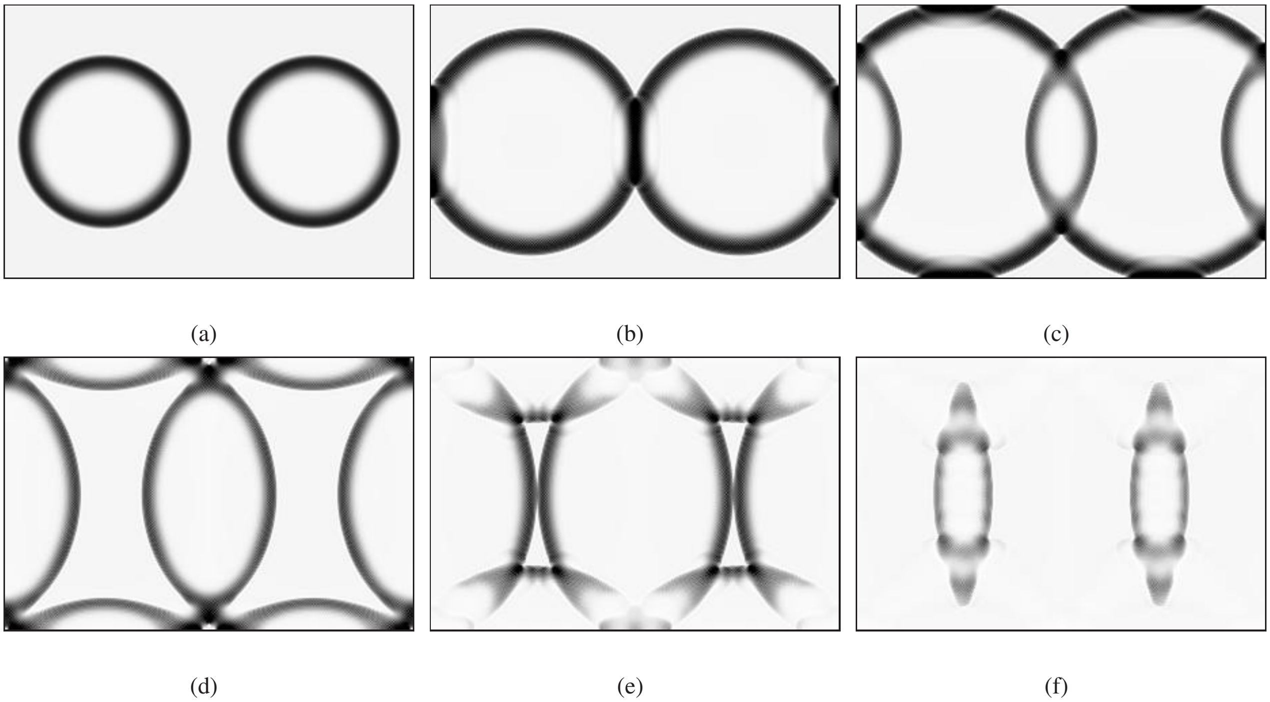

(a) (b) (c)

(d) (e) (f)

FIG. 11: Quasi-soliton interaction of two U-waves with initial radia $R = 70$. Time interval between the panels is 20. Medium size $L_x \times L_y = 150 \times 100$.

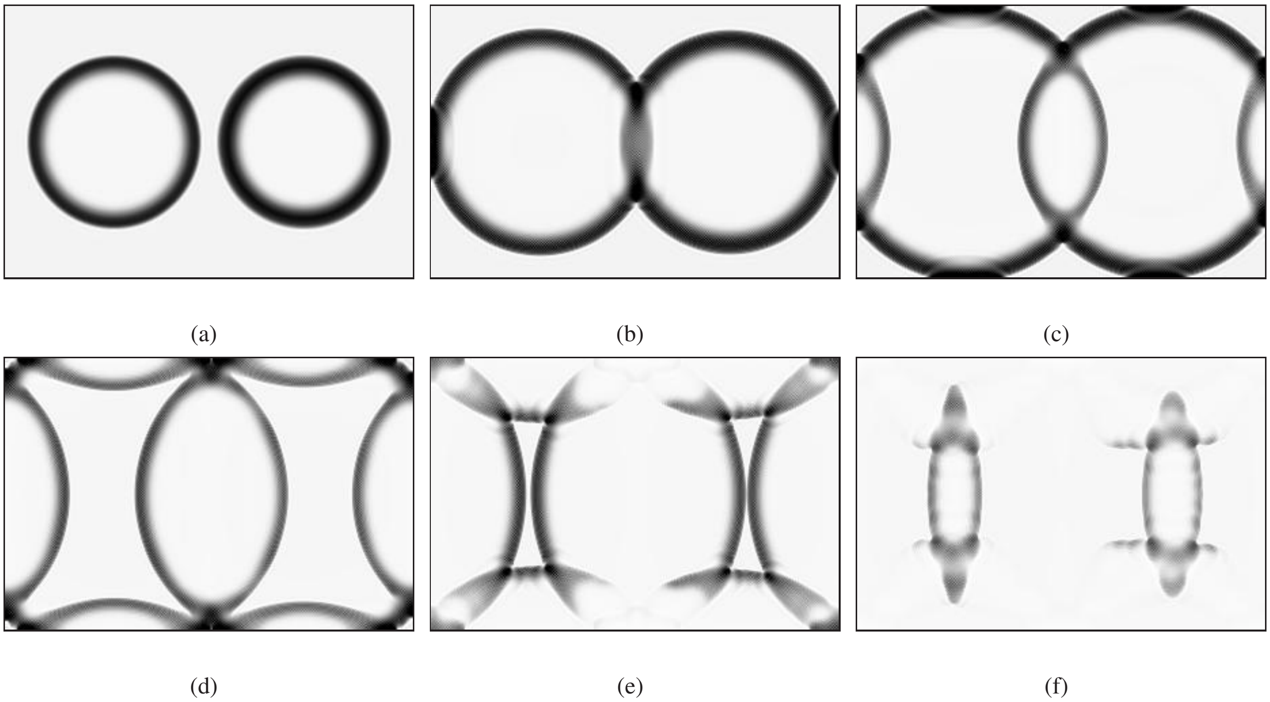

FIG. 12: Quasi-soliton interaction of a U wave and an S wave with initial radia $R = 70$. Time interval between the panels is 20. Domain size $L_x \times L_y = 150 \times 100$.

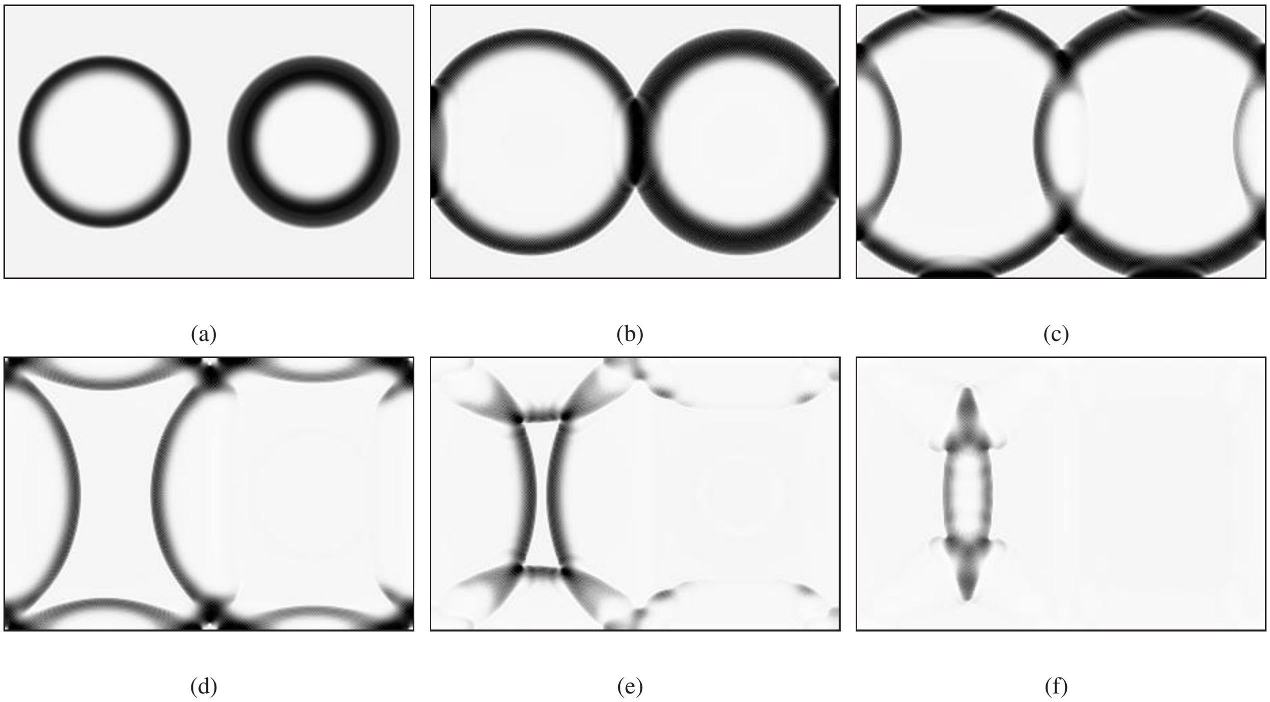

FIG. 13: Half-soliton interaction of a U wave and a W wave with initial radia $R = 70$. Time interval between the panels is 20. Domain size $L_x \times L_y = 150 \times 100$.

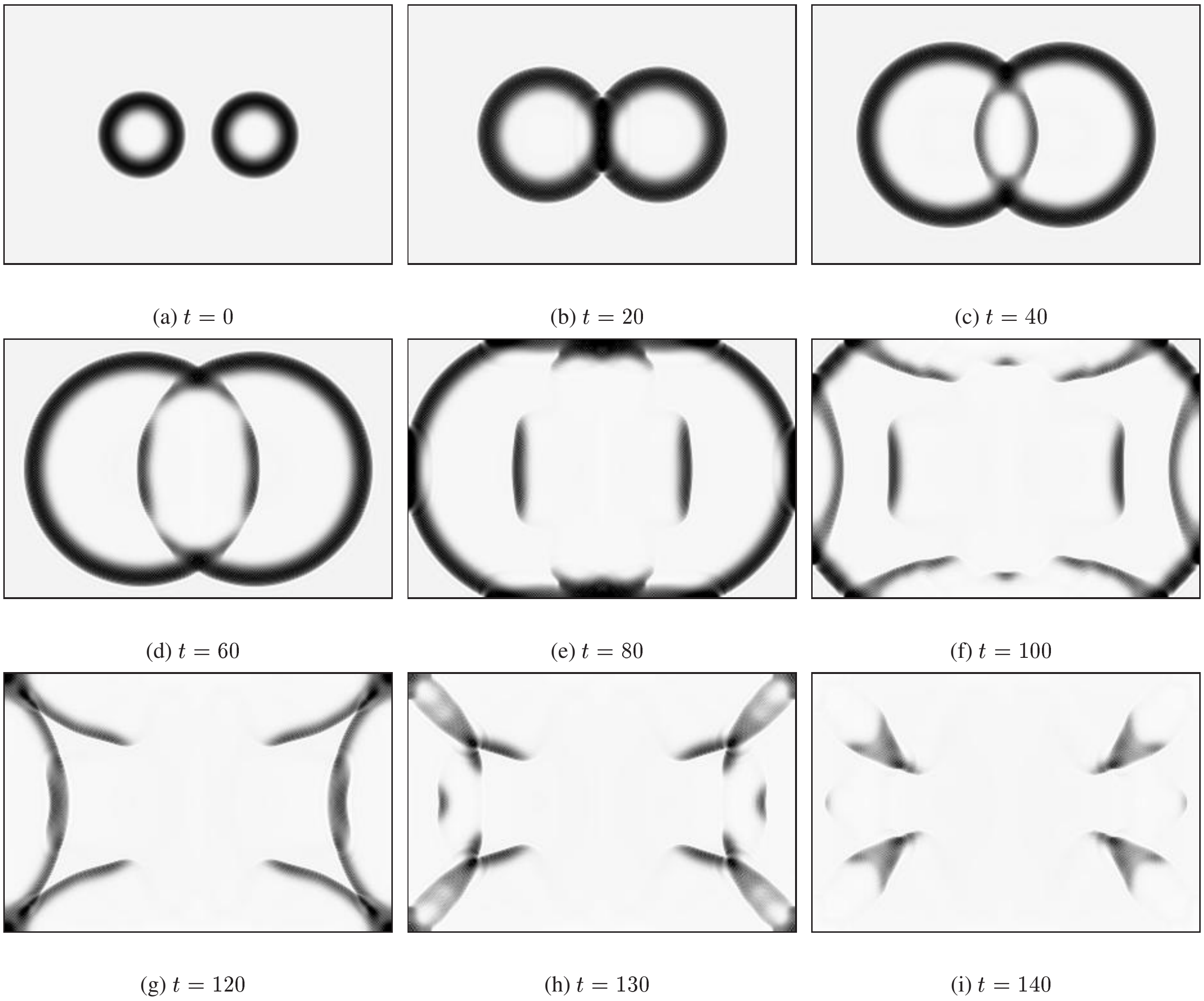

FIG. 14: Interaction of two S-waves with initial radius $R = 40$. Timing is shown under the panels. Domain size $L_x \times L_y = 150 \times 100$.

[1] M. A. Tsyganov, J. Brindley, A. V. Holden, and V. N. Biktashev, Phys. Rev. Lett. **91**, 218102 (2003).

[2] M. A. Tsyganov, J. Brindley, A. V. Holden, and V. N. Biktashev, *Soliton-like phenomena in one-dimensional cross-diffusion systems: a predator-prey pursuit and evasion example* (2004), submitted to Physica D.

[3] V. N. Biktashev, J. Brindley, A. V. Holden, and M. A. Tsyganov, *Pursuit-evasion predator-prey waves in two spatial dimensions* (2004), submitted to Chaos.

[4] E. F. Keller and L. A. Segel, J. Theor. Biol **30**, 225 (1971).

[5] J. E. Truscott and J. Brindley, Philos. Trans. R. Soc. A **347**, 703 (1994).

[6] L. Matthews and J. Brindley, Dyn. Stab. Syst. **12**, 39 (1997).

[7] R. K. Dodd, J. Eilbeck, J. Gibbon, and H. Morris, *Solitons and Nonlinear Waves Equations* (Academic Press, London, 1984).

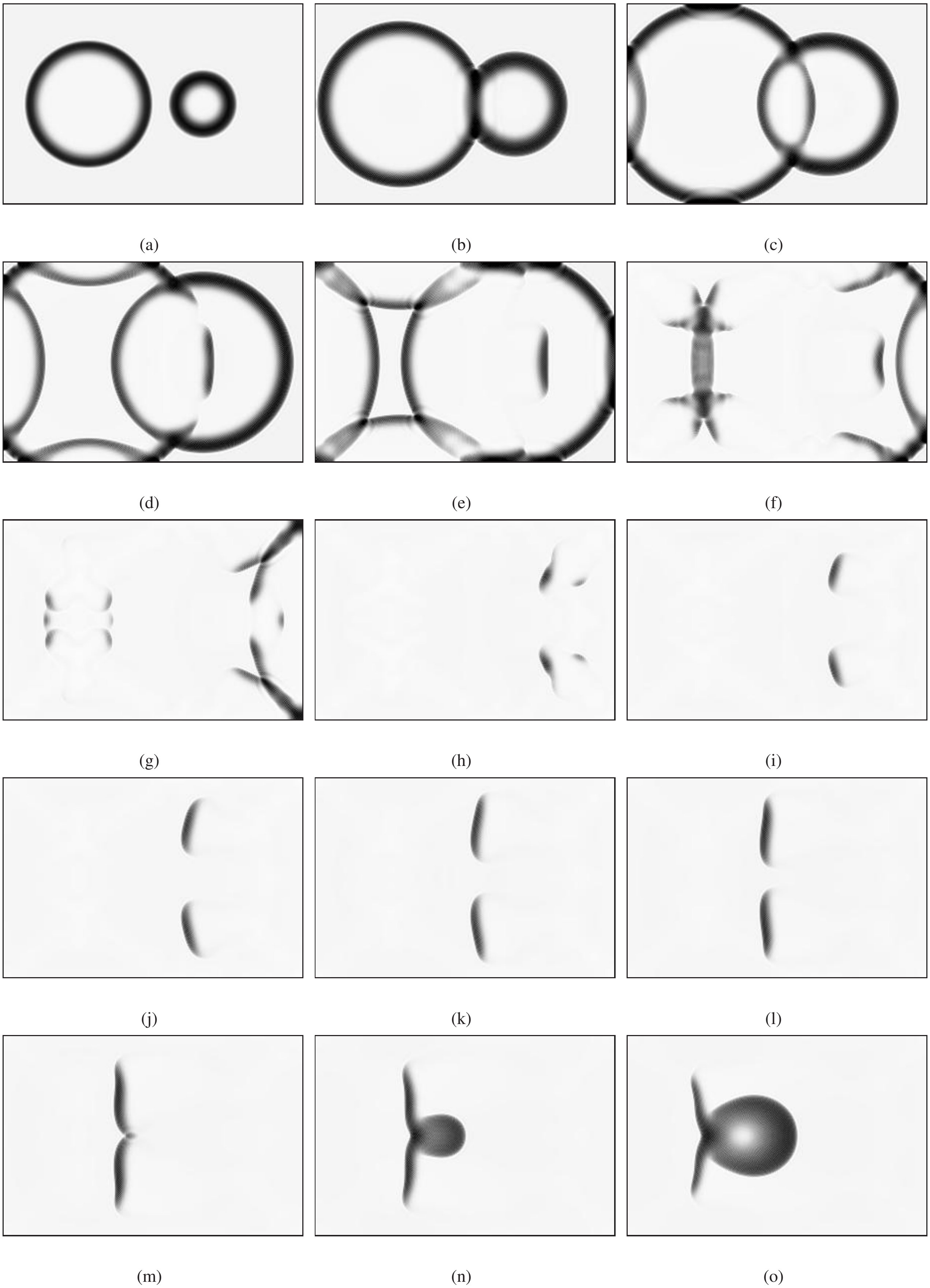

FIG. 15: Interaction of a U wave with initial radius $R = 70$ and an S wave with initiation radius $R = 40$. Time interval between the panels is 20. Domain size $L_x \times L_y = 150 \times 100$.

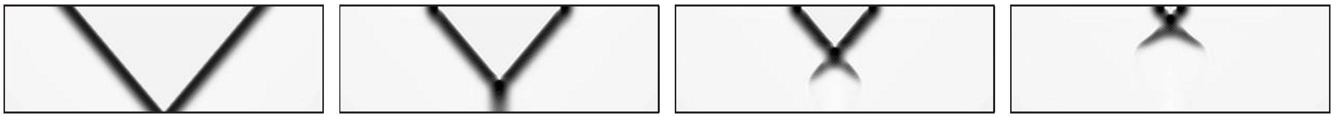

(a) (b) (c) (d)

FIG. 16: Interaction of two plane U waves, with an initial angle of 80° between them. Time interval between the panels is 20. Domain size $L_x \times L_y = 150 \times 50$.

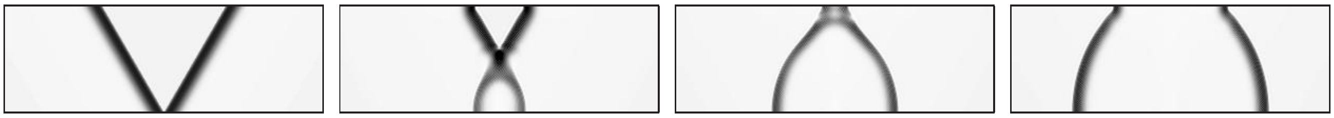

(a) (b) (c) (d)

FIG. 17: Interaction of two plane U waves, with an initial angle of 60° between them. Time interval between the panels is 30. Domain size $L_x \times L_y = 150 \times 50$.

[8] A. von Oertzen, A. S. Mikhailov, H. H. Rotermund, and G. Ertl, J. Phys. Chem. B **102**, 4966 (1998).

[9] O. V. Aslanidi and O. A. Mornev, J. Biol. Phys. **25**, 149 (1999).

[10] J. Adler, Science **153**, 708 (1966).

[11] J. Adler, J. Bacteriol. **92**, 121 (1966).

[12] G. R. Ivanitskii, A. B. Medvinskii, and M. A. Tsyganov, Usp. Fiz. Nauk **161**, 13 (1991).

[13] G. R. Ivanitskii, A. B. Medvinskii, and M. A. Tsyganov, Usp. Fiz. Nauk **164**, 1041 (1994).

[14] K. Agladze, E. Budrene, G. Ivanitsky, V. Krinsky, V. Shakhbazyan, and M. Tsyganov, Proc. R. Soc. London, Ser. B **253**, 131 (1993).

[15] M. A. Tsyganov, I. B. Kresteva, A. B. Medvinskii, and G. R. Ivanitskii, Dokl. Akad. Nauk **333**, 532 (1993).

[16] M. A. Tsyganov, I. B. Kresteva, G. V. Aslanidi, K. B. Aslanidi, A. A. Deev, and G. R. Ivanitsky, J. Biol. Phys. **25**, 165 (1999).

[17] T. Hofer, J. A. Sherratt, and P. K. Maini, Physica (Amsterdam) **85D**, 425 (1995).

[18] B. N. Vasiev, P. Hogeweg, and A. V. Panfilov, Phys. Rev. Lett. **73**, 3173 (1994).

[19] E. O. Budrene and H. Berg, Nature **349**, 630 (1991).

[20] E. O. Budrene and H. Berg, Nature **376**, 49 (1995).

[21] E. Ben-Jacob, O. Schochet, A. Tenenbaum, I. Cohen, A. Czirok, and T. Viscek, Nature **368**, 46 (1994).

[22] M. Mimura, H. Sakaguchi, and M. Matsushita, Physica A **282**, 283 (2000).